

# Photoluminescence properties of blue-emitting $\text{Li}_4\text{SrCa}(\text{SiO}_4)_2:\text{Eu}^{2+}$ phosphor for solid-state lighting

X.M. Zhang · W.L. Li · L. Shi · X.B. Qiao · H.J. Seo

Received: 12 August 2009 / Revised version: 24 October 2009 / Published online: 21 November 2009  
© Springer-Verlag 2009

**Abstract** Blue-emitting  $\text{Li}_4\text{SrCa}(\text{SiO}_4)_2:\text{Eu}^{2+}$  phosphors have been synthesized by solid-state reaction. The photoluminescence (PL) excitation spectrum shows broad-band absorption and matches well with the emission of a near-UV (n-UV) chip. The PL emission spectrum exhibits a broad-band emission peaking at 430 nm, which is the characteristic emission of the f-d transition of the  $\text{Eu}^{2+}$  ion. The diffuse reflection spectra, temperature-dependent emission spectra, fluorescence decay, and mechanism of concentration quenching are also studied in detail.  $\text{Li}_4\text{SrCa}(\text{SiO}_4)_2:\text{Eu}^{2+}$  is a candidate blue phosphor for n-UV excited solid-state lighting.

**PACS** 78.55.-m

## 1 Introduction

Phosphor conversion solid-state lighting, with characteristics of compact size, high efficiency, long lifetime, low power requirement, and energy savings, can be widely used in various applications such as liquid crystal display backlighting, full-color displays, cell phones, and traffic signals [1–3]. White-light-emitting diodes (LEDs), based on

blue LED chips coated with a yellow-emitting phosphor (YAG:Ce) [4], are expected to replace conventional incandescent and fluorescent lamps for general lighting applications in the near future. However, the disadvantage of this system is that since the resulting light is typically deficient in one of the primary colors, lamps fabricated in this manner display a poor color rendering index. White LEDs can also be made by coating near-UV (n-UV) emitting LEDs with a mixture of high-efficiency red, green, and blue emitting phosphors [5, 6]. The visible components of the white light are generated only by phosphors, exhibiting low color point variation against the forward-bias currents.

Silicate is a satisfactory host for rare earth doped phosphors, and some of them have been used widely in industry [7]. The structure of  $\text{Li}_4\text{SrCa}(\text{SiO}_4)_2$  and luminescence properties of  $\text{Eu}^{2+}$ -doped  $\text{Li}_4\text{SrCa}(\text{SiO}_4)_2$  have been studied for the first time by Akella and Keszler [8]. In this paper, we report the luminescent properties of  $\text{Li}_4\text{SrCa}(\text{SiO}_4)_2:\text{Eu}^{2+}$  in detail.  $\text{Li}_4\text{SrCa}(\text{SiO}_4)_2:\text{Eu}^{2+}$  is a promising phosphor for n-UV chip excited solid state lighting.

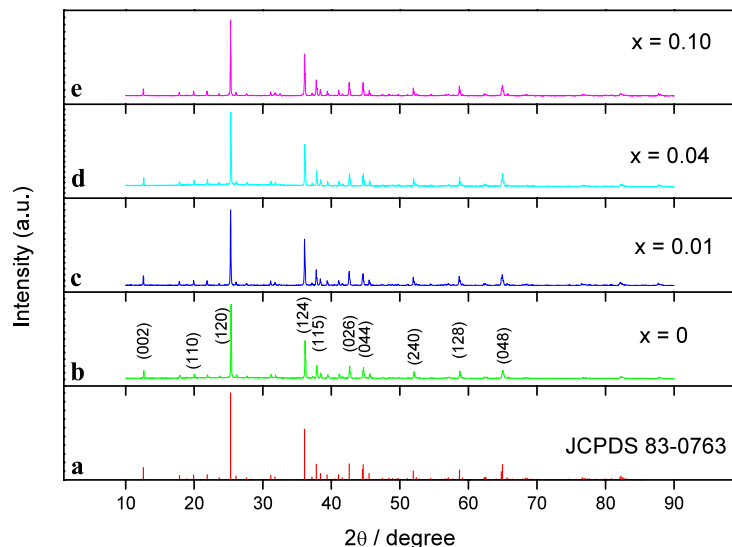
## 2 Experimental

$\text{Li}_4(\text{Sr}_{1-x}\text{Eu}_x)\text{Ca}(\text{SiO}_4)_2$  phosphors were prepared by conventional solid-state reaction. Stoichiometric amounts of source materials  $\text{LiCO}_3$  (Aldrich, 99.99%),  $\text{SrCO}_3$  (Aldrich, 99.99%),  $\text{CaCO}_3$  (Aldrich, 99.99%),  $\text{SiO}_2$  (Aldrich, 99.99%), and  $\text{Eu}_2\text{O}_3$  (Aldrich, 99.99%) were thoroughly mixed and then sintered in air at 600°C for 1 h, and re-sintered in reducing atmosphere ( $\text{N}_2:\text{H}_2 = 95:5$ ) at 1000°C for 12 h. The resulting powder samples were characterized by X-ray powder diffraction (XRD) in the range  $10^\circ \leq 2\theta \leq 90^\circ$  using a D8 Advance diffractometer (Bruker) with

X.M. Zhang · W.L. Li  
School of Materials Science and Engineering, Central South University of Forestry and Technology, Changsha 410004, China  
X.M. Zhang  
e-mail: [zhangxinminam@yahoo.com](mailto:zhangxinminam@yahoo.com)

L. Shi · X.B. Qiao · H.J. Seo (✉)  
Department of Physics, Pukyong National University,  
Busan 608-737, Republic of Korea  
e-mail: [hjseo@pknu.ac.kr](mailto:hjseo@pknu.ac.kr)  
Fax: +82-51-6295549

**Fig. 1** XRD patterns of  $\text{Li}_4(\text{Sr}_{1-x}\text{Eu}_x)\text{Ca}(\text{SiO}_4)_2$  ( $x = 0, 0.01, 0.04$ , and  $0.10$ )



$\text{Cu K}\alpha$  radiation at 40 kV, 30 mA. Diffuse reflectance spectra were taken on a Cary 5000 UV–Vis–NIR spectrophotometer. The photoluminescence (PL) emission and excitation spectra were measured by a Fluorolog-3 fluorescence spectrophotometer with 450-W xenon lamps. Their PL emission spectra at higher temperature were evaluated with a PR-650 SpectraScan spectroradiometer. The luminescence decays were measured by monitoring the given emission from the samples under 355-nm pulsed laser excitation. Decay profiles were recorded with a LeCroy 9301 digital storage oscilloscope in which the signal was fed from a photomultiplier tube.

### 3 Results and discussion

The crystal structure of  $\text{Li}_4\text{SrCa}(\text{SiO}_4)_2$  has been refined to be orthorhombic, space group  $Pbcm$  with  $a = 0.4983(2)$  nm,  $b = 0.9930(2)$  nm, and  $c = 1.4057(2)$  nm [8]. The XRD patterns of  $\text{Li}_4(\text{Sr}_{1-x}\text{Eu}_x)\text{Ca}(\text{SiO}_4)_2$  with  $x = 0, 0.01, 0.04$ , and  $0.10$  are shown in Fig. 1. In this work, we think that the  $\text{Eu}^{2+}$  ions occupy the  $\text{Sr}^{2+}$  ion sites as the two ions show similar ionic radii ( $r_{\text{Sr}}^{2+} = 0.126$  nm,  $r_{\text{Eu}}^{2+} = 0.125$  nm) and the same charge. All the reflections are indexed on the basis of an orthorhombic unit cell of  $\text{Li}_4\text{SrCa}(\text{SiO}_4)_2$  (JCPDS Card: 83-0763). No crystalline impurity phase could be detected in any sample, indicating that the synthesized phosphors are single phase and the doped  $\text{Eu}^{2+}$  ions have no influence on the crystal structure of  $\text{Li}_4\text{SrCa}(\text{SiO}_4)_2$ .

The body color of  $\text{Eu}^{2+}$ -doped  $\text{Li}_4\text{SrCa}(\text{SiO}_4)_2$  phosphors is greyish white. The diffuse reflection spectra of the phosphors were measured and are shown in Fig. 2. It can be seen that there is a distinct absorption band in the range of 250–375 nm, and it becomes stronger gradually with increasing  $\text{Eu}^{2+}$  concentration. This band is assigned to the  $4f$ – $5d$  transition of  $\text{Eu}^{2+}$  ions.

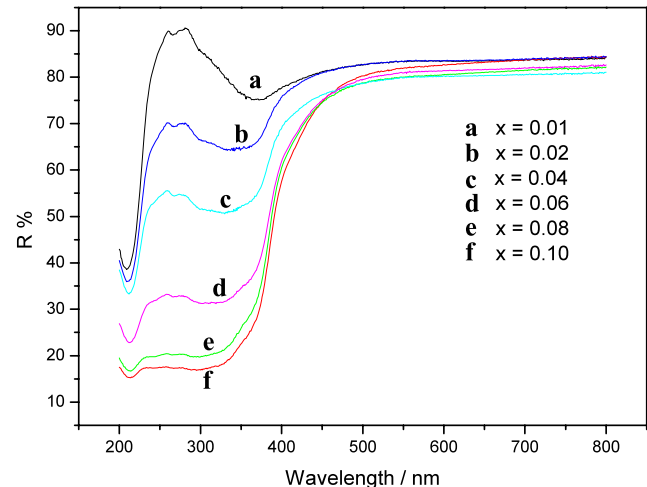


**Fig. 2** Diffuse reflection spectra of  $\text{Li}_4(\text{Sr}_{1-x}\text{Eu}_x)\text{Ca}(\text{SiO}_4)_2$  with different  $\text{Eu}^{2+}$  concentrations

The PL excitation and emission spectra of  $\text{Li}_4(\text{Sr}_{0.96}\text{Eu}_{0.04})\text{Ca}(\text{SiO}_4)_2$  are shown in Fig. 3. The excitation spectrum exhibits a broad absorption from 250 to 400 nm, which is due to  $4f^7 \rightarrow 4f^65d^1$  transitions of  $\text{Eu}^{2+}$  and is consistent with the diffuse reflectance spectra. Because the broad excitation matches well with InGaN chip emission,  $\text{Li}_4(\text{Sr}_{1-x}\text{Eu}_x)\text{Ca}(\text{SiO}_4)_2$  phosphors are suitable for n-UV chip excited solid state lighting. As it has a broad excitation, this phosphor can be excited with different wavelengths. It can be seen from Fig. 3a and b that  $\text{Li}_4(\text{Sr}_{0.96}\text{Eu}_{0.04})\text{Ca}(\text{SiO}_4)_2$  phosphor shows a blue emission band peaking at 430 nm under 280- and 350-nm excitations, which is assigned to the transition from  $4f^65d^1$  to  $4f^7$  of  $\text{Eu}^{2+}$  ions. The full width at half maximum (FWHM) of the emission spectra is 60 nm. The CIE chromaticity coordinates of  $\text{Li}_4(\text{Sr}_{0.96}\text{Eu}_{0.04})\text{Ca}(\text{SiO}_4)_2$  phosphor are cal-

culated in terms of the emission spectrum, and the values are  $x = 0.17$ ,  $y = 0.60$ .  $\text{Eu}^{2+}$  ions exhibit broad-band emission, which is attributed to the  $4f^65d^1-4f^7$  transition, and the wavelength positions of the emission bands depend very much on host, changing from the n-UV to the red. Recently, the PL properties of  $\text{Eu}^{2+}$ -activated  $\text{Li}_2\text{MSiO}_4$  ( $M = \text{Ca}, \text{Sr}, \text{Ba}$ ) phosphors for LEDs have been studied [9–16]. The crystallographic data of  $\text{Li}_2\text{MSiO}_4$  and the emission wavelengths of  $\text{Li}_2\text{MSiO}_4:\text{Eu}^{2+}$  are summarized in Table 1. Although these compounds have similar chemical compositions, their crystal structures are different. The effects of the host structure on luminescence have been explained as arising mainly from two factors, the crystal field effect and the nephelauxetic effect. The center of gravity of the crystal field splitting is affected by the host lattice anion. If the ligand anions share electrons with  $\text{Eu}^{2+}$  ions, the 5d level of  $\text{Eu}^{2+}$  shifts to lower energy. For  $\text{Li}_2\text{MSiO}_4:\text{Eu}^{2+}$  ( $M = \text{Ca}, \text{Sr}, \text{Ba}$ ), only  $\text{O}^{2-}$  anions exist in the crystal struc-

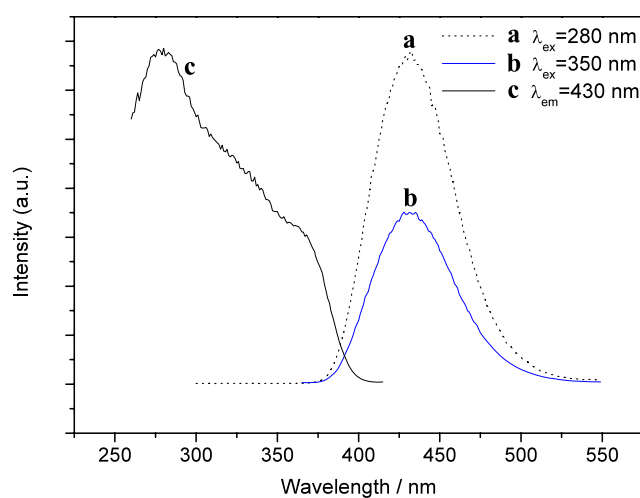


**Fig. 3** PL excitation and emission spectra of  $\text{Li}_4(\text{Sr}_{0.96}\text{Eu}_{0.04})\text{Ca}(\text{SiO}_4)_2$

ture; the shift of emission wavelength does not result from the nephelauxetic effect of  $\text{O}^{2-}$  ions. Therefore, the lowest  $4f^65d^1$  state of the  $\text{Eu}^{2+}$  ion dependence is related to the crystal field strength. In the case of  $\text{A}_{0.5}\text{Zr}_2(\text{PO}_4)_3$  ( $\text{A} = \text{Ca}, \text{Sr}, \text{Ba}$ ), all of them have the NASICON structure. For  $\text{Eu}^{2+}$ -activated  $\text{A}_{0.5}\text{Zr}_2(\text{PO}_4)_3$  ( $\text{A} = \text{Ca}, \text{Sr}, \text{Ba}$ ),  $\text{Eu}^{2+}$  ions have similar bond character to the ligand  $\text{O}^{2-}$  ions; the crystal field splitting becomes large with decreasing Eu–O bond length, leading to a decrease in the difference between the 4f and 5d energy levels in  $\text{Eu}^{2+}$ . The emission bands of  $\text{Eu}^{2+}$  shift from 484 to 435 nm with changing alkaline earth ions from Ca to Ba [17]. However, the crystal field splitting in  $\text{Li}_2\text{MSiO}_4:\text{Eu}^{2+}$  ( $M = \text{Ca}, \text{Sr}, \text{Ba}$ ) is irregular because of different crystal structures [9]. In  $\text{Li}_4\text{SrCa}(\text{SiO}_4)_2:\text{Eu}^{2+}$ , the  $\text{Eu}^{2+}$  site asymmetry leads to strong crystal fields. But, the Stokes shift is small ( $2610 \text{ cm}^{-1}$ ) [18]. The possible mechanism is that the high concentration of  $\text{Li}^+$  ions in the structure constrains the distortion of the emission centers [8, 19]. However, it is not clear at present.

The PL emission spectra of  $\text{Li}_4\text{SrCa}(\text{SiO}_4)_2:\text{Eu}^{2+}$  phosphors as a function of  $\text{Eu}^{2+}$  concentration are shown in Fig. 4. The phosphors show a deep blue emission under 350-nm light excitation, and the emission wavelength does not shift. The emission intensity of  $\text{Li}_4\text{SrCa}(\text{SiO}_4)_2:\text{Eu}^{2+}$  phases as a function of  $\text{Eu}^{2+}$  concentration is shown as an inset in Fig. 4. With increasing  $\text{Eu}^{2+}$  concentration, the emission intensity increases to 0.04 mol of  $\text{Eu}^{2+}$ ; a further increase in the  $\text{Eu}^{2+}$  concentration results in a decrease in the emission intensity because of concentration quenching.

In order to investigate the concentration quenching behavior of the 5d–4f transition emission, the fluorescence decay curves of the 430-nm emission band for  $\text{Li}_4(\text{Sr}_{1-x}\text{Eu}_x)\text{Ca}(\text{SiO}_4)_2$  excited by a pulsed laser ( $\lambda_{\text{ex}} = 355 \text{ nm}$ ) are shown in Fig. 5. The observed decay times significantly shortened with concentration. Moreover, for  $x < 0.04$ , the emission decay is a perfect single-exponential function, whereas for  $x > 0.04$  the decay curves become

**Table 1** Crystallographic data of  $\text{Li}_2\text{MSiO}_4$  ( $M = \text{Ca}, \text{Sr}, \text{Ba}$ ) and emission wavelengths of  $\text{Li}_2\text{MSiO}_4:\text{Eu}^{2+}$

	$\text{Li}_2\text{CaSiO}_4$	$\text{Li}_2\text{SrSiO}_4$	$\text{Li}_2\text{BaSiO}_4$	$\text{Li}_4\text{SrCa}(\text{SiO}_4)_2$
Crystal structure	Tetragonal	Trigonal	Hexagonal	Orthorhombic
Unit cell parameters				
$a/\text{nm}$	0.5047(5)	0.5030(3)	0.8100346	0.4983(2)
$b/\text{nm}$	–	–	–	0.9930(2)
$c/\text{nm}$	0.6484(6)	1.2470(5)	1.0600450	1.4057(2)
Space group	$I\bar{4}2m$	$P3_121$	$P6_3cm$	$Pbcm$
Site symmetry	$\bar{4}2m$	2	$m$	$m(\text{Sr}), 2 (\text{Ca})$
Coordinate number	8 (Ca)	8 (Sr)	9 (Ba)	10 (Sr), 6 (Ca)
Emission wavelength	480 nm ( $\text{Li}_2\text{CaSiO}_4:\text{Eu}^{2+}$ )	560 nm ( $\text{Li}_2\text{SrSiO}_4:\text{Eu}^{2+}$ )	500 nm ( $\text{Li}_2\text{BaSiO}_4:\text{Eu}^{2+}$ )	430 nm ( $\text{Li}_4\text{SrCa}(\text{SiO}_4)_2:\text{Eu}^{2+}$ )
References	[9, 15]	[9, 13, 14, 16]	[9]	This work, [8]

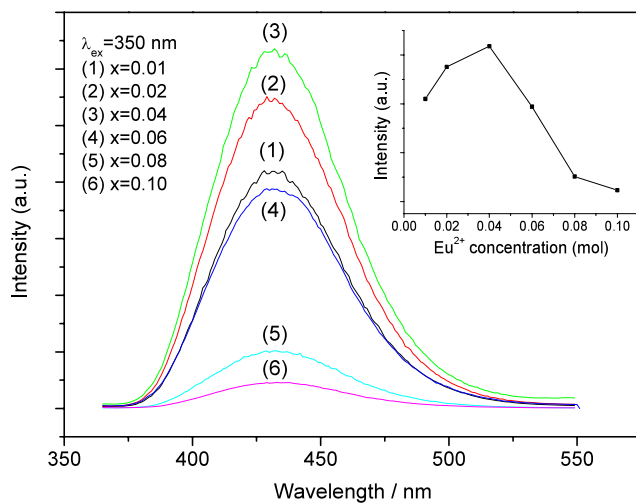


**Fig. 4** PL emission spectra of  $\text{Li}_4(\text{Sr}_{1-x}\text{Eu}_x)\text{Ca}(\text{SiO}_4)_2$  (the inset shows the dependence of PL intensity on  $\text{Eu}^{2+}$  concentration)

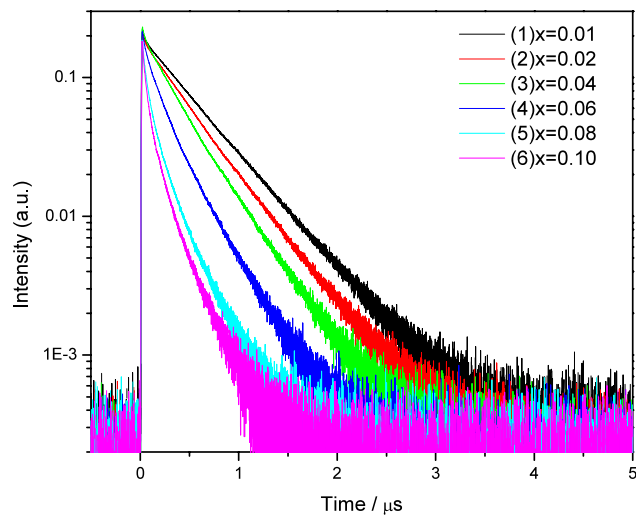


**Fig. 5** Decay curves of  $\text{Li}_4(\text{Sr}_{1-x}\text{Eu}_x)\text{Ca}(\text{SiO}_4)_2$  phosphor ( $\lambda_{\text{ex}} = 355 \text{ nm}$ ,  $\lambda_{\text{em}} = 430 \text{ nm}$ )

nonexponential and the nonexponential is becoming more prominent with increasing  $\text{Eu}^{2+}$  concentration. The deviation from the single-exponential behavior has been shown to be due to the nonradiative energy transfer process involving  $\text{Eu}^{2+}$  ions and defect impurities [20]. The analysis of these decay curves shows that energy migration among  $\text{Eu}^{2+}$  ions affects the energy transfer process [20, 21]. The fit of the fluorescence decays of higher doped samples with the migration assisted energy transfer modes from Yokota and Tanimoto [22] and Burshtein [23] indicates that the best agreement between experimental data and theoretical fits is obtained with the expression corresponding to the Burshtein model

$$I(t) = I_0 \exp\left(-\frac{t}{\tau_R} - \gamma\sqrt{t} - Wt\right), \quad (1)$$

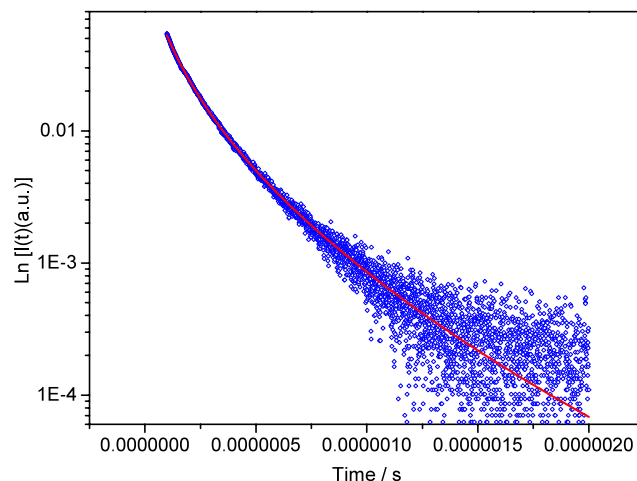


**Fig. 6** Experimental emission decay curves of  $\text{Li}_4(\text{Sr}_{0.90}\text{Eu}_{0.10})\text{Ca}(\text{SiO}_4)_2$  and the calculated fit with (1) (solid line)

where  $\tau_R$  is the intrinsic lifetime of the donor ions,  $\gamma$  characterizes the direct energy transfer, and  $W$  represents the migration parameter. In the case of dipole–dipole interaction,  $\gamma$  is given by the expression  $\gamma = \frac{4}{3}\pi^3/2NC_{\text{DA}}^{1/2}$ , where  $N$  is the concentration and  $C_{\text{DA}}$  is the energy transfer microparameter. Figure 6 shows the fit for the sample  $\text{Li}_4(\text{Sr}_{0.90}\text{Eu}_{0.10})\text{Ca}(\text{SiO}_4)_2$  phosphor.

The result indicates that the electronic mechanism of energy transfer is a dipole–dipole interaction between  $\text{Eu}^{2+}$  ions. For the  $\text{Li}_4(\text{Sr}_{0.90}\text{Eu}_{0.10})\text{Ca}(\text{SiO}_4)_2$  phosphor, the  $\text{Eu}^{2+}$  concentration  $N = 5.75 \times 10^{20} \text{ cm}^{-3}$ . The  $\gamma$  value is determined to be 5947. So, the calculated  $C_{\text{DA}} = 1.94 \times 10^{-36} \text{ cm}^6/\text{s}$ . The critical distance  $R_0$  calculated by  $R_0^6 = \tau_R C_{\text{DA}}$  is 9.95 Å, which is smaller than 20 Å that is usually observed in other phosphors, and is consistent with the concentration quenching occurring at low doping levels in  $\text{Li}_4\text{SrCa}(\text{SiO}_4)_2:\text{Eu}^{2+}$ .

Thermal quenching is one of the important technological parameters for phosphors used in solid-state lighting. The temperature dependence of PL emission spectra of  $\text{Li}_4\text{Sr}_{0.96}\text{Ca}(\text{SiO}_4)_2:0.04\text{Eu}^{2+}$  excited by 365-nm UV light is illustrated in Fig. 7. With increasing temperature, the emission intensity decreases markedly. When the temperature is 150°C at which the solid-state lighting usually works, the emission intensity remains only 55% of that at room temperature, which can be explained by the thermal quenching at the configurational coordinate diagram. Through phonon interaction, the excited luminescent center is thermally activated and then released through the crossing point between the excited state and the ground state in the configurational coordinate diagram [7, 24], which quenches the luminescence. In addition, a slight blue shift from 430 to 425 nm is observed with increasing temperature from 25 to 200°C. This blue shift can be explained in terms of the thermally active phonon assisted excitation from a lower energy sublevel

**Fig. 7** Dependence of PL emission of  $\text{Li}_{0.96}\text{SrCa}(\text{SiO}_4)_2:0.04\text{Eu}^{2+}$  on temperature (the inset shows the relation between the relative intensity and temperature)

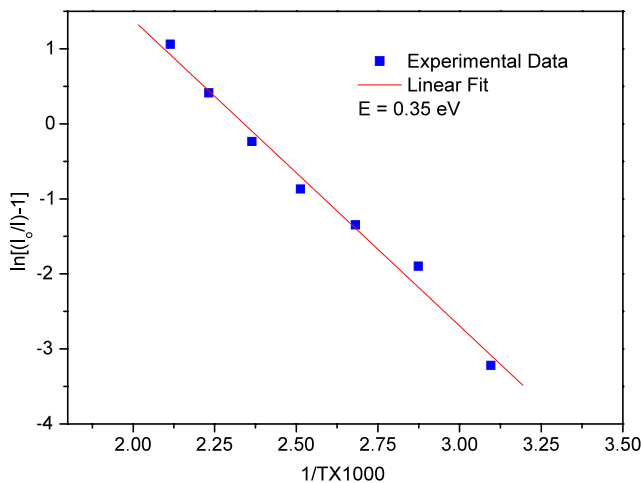
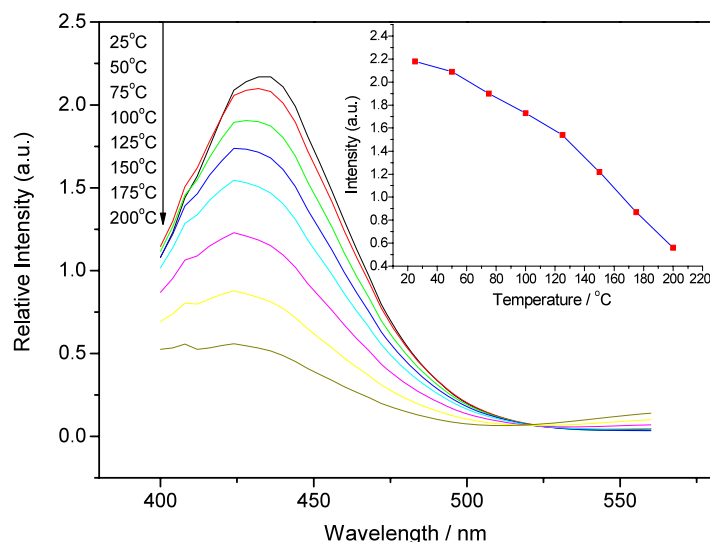


**Fig. 8** Activation energy for thermal quenching of  $\text{Li}_{0.96}\text{SrCa}(\text{SiO}_4)_2:0.04\text{Eu}^{2+}$

to a higher energy sublevel in the excited state of  $\text{Eu}^{2+}$  [7]. This temperature-induced blue shift phenomenon has been reported by many authors [25–28].

In order to better understand the relationship between temperature and photoluminescence and to determine the activation energy for thermal quenching, the Arrhenius equation was fitted to the thermal quenching data [25, 29]:

$$I(T) = \frac{I_0}{1 + c \exp\left(\frac{-E}{kT}\right)}, \quad (2)$$

where  $I_0$  is the initial intensity,  $I(T)$  is the intensity at a given temperature  $T$ ,  $c$  is a constant,  $E$  is the activation energy for thermal quenching, and  $k$  is Boltzmann's constant. Figure 8 plots  $\ln[(I_0/I) - 1]$  vs.  $1/T$ . When performing linear regression, the activation energy for thermal quenching is found to be 0.35 eV.

#### 4 Conclusions

Single-phase  $\text{Li}_4\text{SrCa}(\text{SiO}_4)_2:\text{Eu}^{2+}$  phosphors have been synthesized by solid-state reaction. The absorption band in the range of 250–375 nm in the diffuse reflection spectra is assigned to the 4f–5d transition of the  $\text{Eu}^{2+}$  ion. The PL excitation spectrum shows broad-band absorption extending to the n-UV region and is consistent with the diffuse reflectance spectra. The PL emission spectrum exhibits a broad-band emission peaking at 430 nm, which is the characteristic emission of the f–d transition of the  $\text{Eu}^{2+}$  ion. The optimum  $\text{Eu}^{2+}$  doping concentration is 4 mol%. The concentration quenching is made evident by the change from exponential to nonexponential decays of the  $\text{Eu}^{2+}$  d–f transition emission with increasing doping concentration. The study of decay curves indicates that the electronic mechanism of energy transfer is a dipole–dipole interaction between  $\text{Eu}^{2+}$  ions. The emission intensity decreases with temperature increasing, and the emission intensity at 150°C remains at 55% of that at room temperature. Because the PL excitation of  $\text{Li}_4\text{SrCa}(\text{SiO}_4)_2:\text{Eu}^{2+}$  phosphors matches well with the emission of an n-UV chip,  $\text{Li}_4\text{SrCa}(\text{SiO}_4)_2:\text{Eu}^{2+}$  phosphor is a promising blue component for n-UV excited solid-state lighting.

**Acknowledgements** This work was supported by the Pukyong National University Research Fund in 2009 (PK-2009-24). This work was also supported by the Scientific Research Foundation for Advanced Talents of Central South University of Forestry and Technology, under Grant No. 07Y023.

#### References

1. S. Chawla, N. Kumar, H. Chander, J. Lumin. **129**, 114 (2009)
2. R. Zheng, J. Light Vis. Environ. **32**, 230 (2008)

3. K. Inoue, N. Hirosaki, R.J. Xie, T. Takeda, *J. Phys. Chem. C* **113**, 9392 (2009)
4. K. Yamada, Y. Imai, K. Ishii, *J. Light Vis. Environ.* **27**, 70 (2003)
5. X.M. Zhang, H. Chen, W.J. Ding, H. Wu, J.S. Kim, *J. Am. Ceram. Soc.* **92**, 429 (2009)
6. H. Sakuta, T. Fukui, T. Miyachi, K. Kamon, H. Hayashi, N. Nakamura, Y. Uchida, S. Kurai, T. Taguchi, *J. Light Vis. Environ.* **32**, 39 (2008)
7. S. Shionoya, W.M. Yen, *Phosphor Handbook* (CRC, Berlin, 1999)
8. A. Akella, D.A. Keszler, *Inorg. Chem.* **34**, 1308 (1995)
9. C. Kulshreshtha, A.K. Sharma, K.S. Sohn, *J. Electrochem. Soc.* **156**, J52 (2009)
10. C. Kulshreshtha, N. Shin, K.S. Sohn, *Electrochem. Solid-State Lett.* **12**, J55 (2009)
11. X.L. Zhang, H. He, Z.S. Li, T. Yu, Z.G. Zou, *J. Lumin.* **128**, 1876 (2008)
12. H. He, R.L. Fu, H. Wang, X.F. Song, Z.W. Pan, X.R. Zhao, X.L. Zhang, Y.G. Cao, *J. Mater. Res.* **23**, 3288 (2008)
13. K. Toda, Y. Kawakami, S. Kousaka, Y. Ito, A. Komeno, K. Uematsu, M. Sato, *IEICE Trans. Electron. E* **89**, 1406 (2006)
14. M.P. Saradhi, U.V. Varadaraju, *Chem. Mater.* **18**, 5267 (2006)
15. J. Liu, H.Y. Sun, C.S. Shi, *Mater. Lett.* **60**, 2830 (2006)
16. B. Haferkorn, G. Meyer, *Z. Anorg. Allg. Chem.* **624**, 1079 (1998)
17. M. Hirayama, N. Sonoyama, A. Yamada, R. Kanno, *J. Solid State Chem.* **182**, 730 (2009)
18. P. Dorenbos, *J. Lumin.* **104**, 239 (2003)
19. G. Blasse, *J. Solid State Chem.* **27**, 3 (1979)
20. K.B. Eisenthal, S. Siegel, *J. Chem. Phys.* **41**, 652 (1964)
21. M. Inokuti, F. Hirayama, *J. Chem. Phys.* **43**, 1978 (1965)
22. M. Yokota, O. Tanimoto, *J. Phys. Soc. Jpn.* **22**, 779 (1967)
23. A.I. Burshtein, *Sov. J. Exp. Theor. Phys.* **35**, 882 (1972)
24. J.S. Kim, Y.H. Park, S.M. Kim, J.C. Choi, H.L. Park, *Solid State Commun.* **133**, 445 (2005)
25. R.J. Xie, N. Hirosaki, N. Kimura, K. Sakuma, M. Mitomo, *Appl. Phys. Lett.* **90**, 191101 (2007)
26. W.J. Ding, J. Wang, M. Zhang, Q.H. Zhang, Q. Su, *Chem. Phys. Lett.* **435**, 301 (2007)
27. Y.Q. Li, H.T. Hintzen, *J. Light Vis. Environ.* **32**, 129 (2008)
28. J. Liu, Z. Wu, M. Gong, *Appl. Phys. B, Lasers Opt.* **93**, 583 (2008)
29. C.C. Lin, R.S. Liu, Y.S. Tang, S.F. Hu, *J. Electrochem. Soc.* **155**, J248 (2008)